Electrochemical Extraction of Nd from NaCl-KCl Melt by Formation of Cu-Nd Alloys

ZHONG-LIN ZHANG, LIN-ZONG ZHOU, DE-BIN JI, YONG-DE YAN, WEI HONG, YU-HUI LIU, PU WANG, TAI-QI YIN, JIA-NING ZHENG, YUN XUE, and YUAN-FENG YE

Electrochemical behavior of Nd was studied in NaCl-KCl melt on W and Cu electrodes *via* cyclic voltammetry and chronopotentiometry. Generally, the reduction of Nd^{3+} takes place in two consecutive steps in molten chlorides, such as LiCl-$CaCl_2$, LiCl-$BaCl_2$, $CaCl_2$-NaCl, LiCl-KCl melts. However, the reduction of Nd^{3+} ions was found to be through a one-step process: $Nd^{3+} + 3e^- \rightarrow Nd$. The co-reduction behavior of Nd^{3+} and Cu^{2+} ions and the mechanisms of alloy formation were investigated in NaCl-KCl melt on W electrodes at 988 K (715 °C). Four potential plateaus corresponding to four different kinds of Cu-Nd intermetallic compounds were detected. Cu-Nd alloys were prepared on Cu electrodes at 988 K (715 °C) and 1143 K (870 °C). At 988 K (715 °C), Cu_5Nd phase was identified by X-ray diffraction. The morphology and micro-zone chemical analysis of the alloys were characterized by scanning electron microscopy equipped with energy-dispersive spectrometry. The alloy film was observed on the Cu electrodes. Moreover, at 1143 K (870 °C), a globate bulk Cu-Nd alloy with Cu_5Nd, Cu_4Nd, Cu_2Nd, CuNd, and Cu phases, as liquid in the melt, was obtained at the bottom of the crucible.

DOI: 10.1007/s11663-017-1017-6

I. INTRODUCTION

FULL recovery and reasonable treatment of spent nuclear fuel are key concerns for future nuclear power stations. To reduce the output and long-lived radiotoxicity of spent fuel and high-level waste, partitioning and transmutation (P&T) strategies have become a potential option for the advanced fuel cycle and an alternative for complementary waste management.[1] The first requirement of P&T is to extend the performance of Pu separation to 99.9 pct, separating Np, Am, and Cm, either as a group or individually, and in any case to remove lanthanide (Lns) contaminates as much as possible. The separated transuranium elements (TRUs) should then be ''transmuted'' (or ''burned'') in a neutron field.[2] However, Lns can effectively absorb neutrons and prevent neutron capture by TRUs. Therefore, TRUs have to be separated from Lns to avoid affecting their transmutation efficiency; molten salts employed as solvent media have been proposed as a promising option to achieve this.[3] On the other hand, the accumulation of Lns in the molten salts will modify their physical and chemical properties and contaminate the final cathodic product. When Lns concentration exceeds about 10 wt pct in the melt it must generally be regenerated to avoid lowering the TRUs/Lns separation efficiency[4] and to recycle the molten salts, because the reprocessing agent should be stable and immediately available for reuse, without further treatment.[5]

Molten chlorides are reported to be convenient solvents for obtaining the detailed chemistry of fission products in molten salts due to their high radiation and thermal resistance, low neutron cross section, and high solubility of fuel components.[5] Nd is abundant in the fission products with a large transverse section of neutron capture and is one of the surrogate elements of Am^{3+} in molten salts.[6–8] The electrochemical behavior of Nd^{3+} has been widely studied in molten chloride. The reduction of Nd^{3+} takes place in two consecutive steps in LiCl-$CaCl_2$, LiCl-$BaCl_2$, $CaCl_2$-NaCl, LiCl-KCl melts.[6,9–12] In molten chlorides, like other valence Lns (Sm, Eu, Tm, and Yb), Nd has two stable electro-active forms, Nd^{2+} and Nd^{3+}. However, for Nd and Tm, they are a little different from Sm, Eu, and Yb. This is because the deposition potentials of Nd^{2+} and Tm^{2+} are more positive than those of

ZHONG-LIN ZHANG, DE-BIN JI, YONG-DE YAN, WEI HONG, YU-HUI LIU, PU WANG, TAI-QI YIN, JIA-NING ZHENG, and YUN XUE are with the Harbin Engineering University, Harbin 150001, China. Contact e-mails: jidebin@hrbeu.edu.cn, y5d2006@hrbeu.edu.cn LIN-ZONG ZHOU is with the Chu Xiong Normal University, Chuxiong 675000, China. YUAN-FENG YE is with the Jinling Institute of Technology, Nanjing 211169, China.

Manuscript submitted November 9, 2015.
Article published online July 18, 2017.

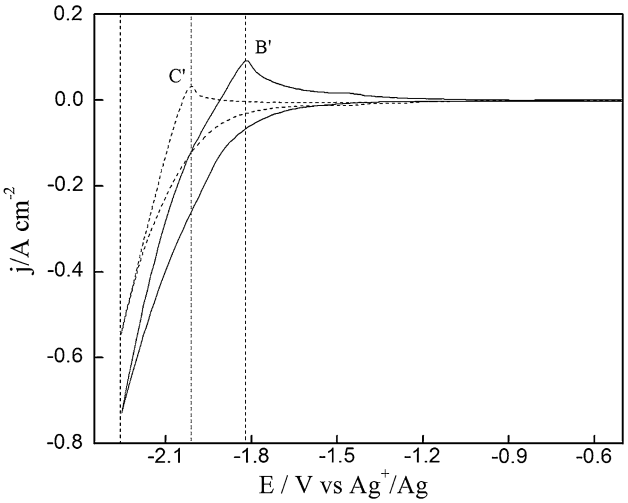

Fig. 1—Cyclic voltammograms obtained at a W electrode (S = 0.32 cm^2) in NaCl-KCl melt before (dotted line) and after (solid line) the addition of 2 wt pct $NdCl_3$ at 988 K (715 °C).

common solvents (Li^+, Na^+, and K^+) while those of Sm^{2+}, Eu^{2+}, and Yb^{2+} are closer to or more negative than common solvents. Therefore, it is possible to deposit Nd and Tm on an inert electrode in common solvents. However, corrosion reactions occur between Nd(Tm) metal and Nd^{3+}(Tm) in the molten chloride media, which are expressed as follows: $2Nd^{3+} + Nd \leftrightarrow 3Nd^{2+}$. Taking this into account, if the preparation of metal Tm(Nd) is carried out on inert electrodes, a low current yield in the electrolysis and a low stability of the deposits are expected.[13] Therefore, employing electro-reduction of Nd^{3+} on a reactive electrode to extract Nd seems to be a sensible choice because alloy formation can prevent the corrosion reaction.

Interestingly, Nohira and colleagues[14] have reported that Nd^{3+} reduction was by a one-step process with a three-electron exchange in NaCl-KCl melt. They prepared different phases of Ni-Nd alloys ($NdNi_2$, $NdNi_3$, Nd_2Ni_7, and $NdNi_5$) on Ni electrodes and determined the corresponding equilibrium potentials. However, so far, only a one-step Nd^{3+} reduction has been reported in molten fluoride, such as LiF-CaF_2, LiF-NaF, LiF-$CaCl_2$, and LiF melts.[3,15–17] Massot and colleagues[18] have investigated the co-reduction process of Al-Nd alloys in LiF-CaF_2 melt (79 to 21 mol. pct) on an inert W electrode. Extraction of Nd was performed *via* potentiostatic electrolysis with an efficiency of about 95 pct. In addition, they[3,19] have investigated Nd^{3+} reduction on Cu and Ni electrodes in LiF-CaF_2 melt. Cu is considered to be a better cathode material than Ni, for their experimental temperature 988 K (715 °C), Cu and Nd form liquid intermetallic compounds. As the kinetics of the alloy layer growth is controlled by the intermetallic diffusion within the surface alloy layer,[3] liquid alloy formation can keep the surface of the cathode free of diffusion layer.

Therefore, this paper is concerned with the electrochemical behavior of Nd^{3+} in NaCl-KCl melt and its reduction mechanism on W and Cu electrodes, respectively.

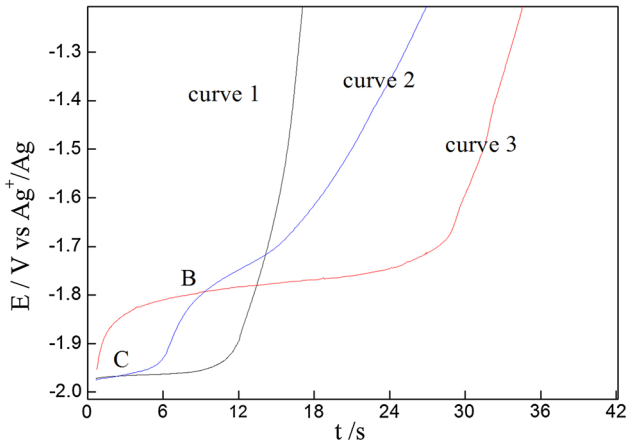

Fig. 2—Open circuit chronopotentiometry curves obtained on a W electrode (S = 0.32 cm^2) at 988 K (715 °C) in NaCl-KCl melt after potentiostatic electrolysis at −2.3 V for 10 s (curve 1); in NaCl-KCl-$NdCl_3$ (2 wt pct) melt after potentiostatic electrolysis at −2.3 V for 10 s (curve 2); in NaCl-KCl-$NdCl_3$ (2 wt pct) melt after potentiostatic electrolysis at −2.0 V for 60 s (curve 3), respectively.

II. EXPERIMENTAL

NaCl-KCl melt (99.5 pct NaCl, 99.5 pct KCl, and mole ratio of sodium to potassium = 50.6:49.4 pct) was dried under vacuum for more than 72 hours at 473 K (200 °C) to remove excess H_2O before being used. Cu^{2+} and Nd^{3+} ions were introduced into NaCl-KCl melt in the form of anhydrous $CuCl_2$ (99.5 pct) and $NdCl_3$ (Aladdin Chemistry Co. Ltd. ≥99.95 pct) powder, respectively. All experiments were carried out in an inert atmosphere which was maintained by purging with purified Ar gas to avert exposure to O_2 and H_2O.

Cyclic voltammetry, chronopotentiometry, and galvanostatic electrolysis tests were performed using an Autolab PGSTAT302N potentiostat/galvanostat controlled with the Nova 1.8 software package. The transient electrochemical measurements were carried out in an electrochemical quartz cell with a three-electrode setup. The working electrodes were W wire (d = 1 mm), Cu wire (d = 2 mm), and Cu plate (10 mm × 10 mm × 0.2 mm). The lower ends of the working electrodes were polished thoroughly with SiC paper and then cleaned in ethanol using ultrasound to remove the oxide film and impurities on the electrode surface. The active surface area of working electrode was determined after each experiment by measuring the immersion depth of the electrode. The counter electrode was a spectral pure graphite rod (d = 6 mm). Ag^+/Ag couple was used as reference electrode, which consisted of AgCl (1.0 wt pct) in NaCl-KCl molten mixture. The temperature of the melts was measured with a chromel–alumel thermocouple.

Cu-Nd alloys were prepared *via* galvanostatic electrolysis on Cu electrodes. After electrolysis, the samples were washed with ethylene glycol to remove solidified salts attached on the surface of the alloy samples. Then the deposits were successively polished with 360#, 600#, 1500#, and 2000# metallographic emery papers to make a cross section. The samples were analyzed by X-ray

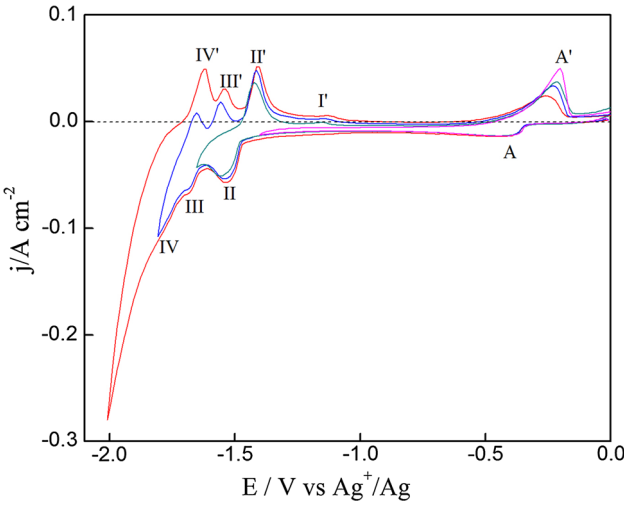

Fig. 3—Cyclic voltammograms obtained at a W electrode (S = 0.32 cm^2) in NaCl-KCl-1 wt pct $CuCl_2$-2 wt pct $NdCl_3$ melt at different reversal potentials at 988 K (715 °C).

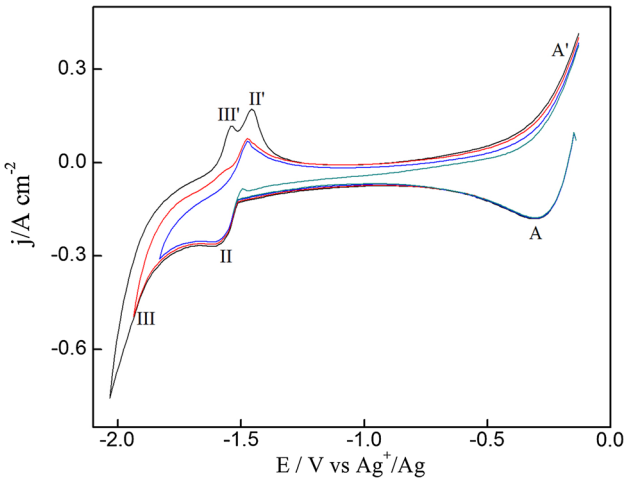

Fig. 4—Cyclic voltammograms obtained at a Cu electrode (S = 0.32 cm^2) in NaCl-KCl-2 wt pct $NdCl_3$-1 wt pct $CuCl_2$ melt at different reversal potentials at 988 K (715 °C).

diffraction (XRD) (Rigaku D/max-TTR-III diffractometer) using Cu Kα radiation at 40 kV and 150 mA. Scanning electron microscopy (SEM) equipped with energy-dispersive spectrometry (EDS) (JSM-6480A; JEOL Co., Ltd.) was used to analyze the microstructure and micro-zone chemical composition of bulk Cu-Nd alloys.

III. RESULTS AND DISCUSSION

A. *Electrochemical Behavior of Nd^{3+} on a W Electrode*

Figure 1 exhibits cyclic voltammograms obtained on a W electrode in NaCl-KCl melt before (dotted line) and after (solid line) the addition of 2 wt pct $NdCl_3$ at 988 K (715 °C). In NaCl-KCl melt, the cathodic limit is related to the formation/dissolution of metal Na. It is noteworthy that the reduction current corresponding to Na deposition is much larger than the reoxidation current. The reason is that some deposited Na dissolved in the melt and Na fog is formed in the cathodic process. After the addition of Nd^{3+}, compared to the dotted line, the solid line shows that the reduction of Nd^{3+} starts at around −1.70 V, which makes the larger reduction current at potentials more negative than −1.70 V. In the anodic direction, only signal B′, which peaks at about −1.82 V, is observed, and is thought to be related to the dissolution of Nd because the peak potential of signal B′ in the solid line is about 0.2 V more positive than that of signal C′ in the dotted line related to the oxidation of Na. The reason for the absence of Na dissolution signal is that the deposited Nd in the working electrode accelerates the dissolution of metal Na in the melt. Therefore, on the basis of the above discussion, the reduction of Nd^{3+} in NaCl-KCl melt was through a one-step process. The reaction is thought to be as follows: $Nd^{3+} + 3e \rightarrow Nd$. In other molten chlorides, Nd^{3+} reduction was through two consecutive steps. The reason for one-step reduction of Nd^{3+} in NaCl-KCl melt is that Nd^{2+} is not stable in NaCl-KCl melt due to its disproportionate reaction in molten chlorides: $3Nd^{2+} \rightarrow 2Nd^{3+} + Nd$. Castrillejo *et al.*[20] have reported that the stability of Nd^{2+} is related to molten salt systems. Therefore, there may be almost no Nd^{2+} ions in NaCl-KCl melt, or the concentration probably is very low.

Open circuit chronopotentiometry was employed to further study the Nd^{3+} reduction. Figure 2 shows open circuit chronopotentiometry curves obtained on the W electrode in NaCl-KCl melt before (curve 1) and after (curves 2 and 3) the addition of $NdCl_3$ at 988 K (715 °C). In NaCl-KCl melt (curve 1), only plateau C at about −1.97 V is detected corresponding to the reduction of Na^+. After the addition of $NdCl_3$, apart from the plateau C, a new plateau B is observed, which is attributed to the reduction of Nd^{3+} to Nd *via* a one-step process. Curve 3 illustrates the open circuit chronopotentiometry curve obtained in NaCl-KCl-$NdCl_3$ (2 wt pct) melt on a W electrode after potentiostatic electrolysis at −2.0 V for 60 seconds. Therefore, the Na^+ reduction plateau disappears, and only one potential plateau B corresponding to the reduction of Nd^{3+} can be observed.

Based on the above discussion, the potential gap (ΔE) between the reduction of Nd^{3+} and solvent Na^+ ions is about 0.14, which suggests that the extraction of Nd^{3+} from NaCl-KCl melt on inert electrode is feasible. However, ΔE is not large enough to achieve complete extraction as required for recycling.[3] One way to successfully eliminate Nd^{3+} ions from the molten salt is to increase ΔE. Therefore, in our paper, we employ two methods to increase ΔE: (i) co-reduction of Cu^{2+} and Nd^{3+} *via* the formation of Cu-Nd intermetallic compounds on an inert W electrode; (ii) electro-reduction of Nd^{3+} on a Cu electrode.

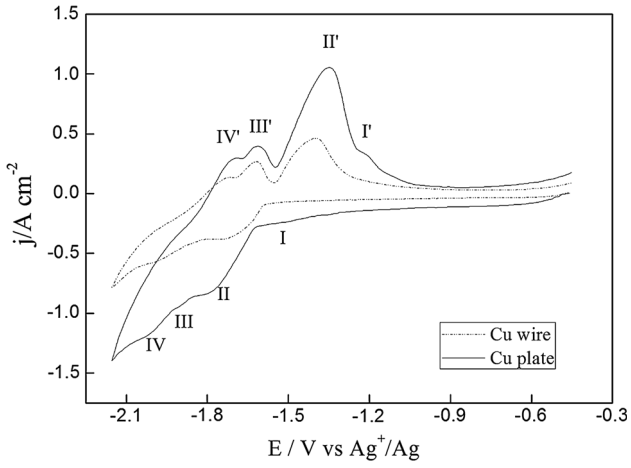

Fig. 5—Cyclic voltammograms obtained at 988 K (715 °C) in NaCl-KCl-4 wt pct $NdCl_3$ at a Cu wire (S = 0.32 cm^2, dotted line) and plate (S = 1.00 cm^2, solid line) electrodes, respectively.

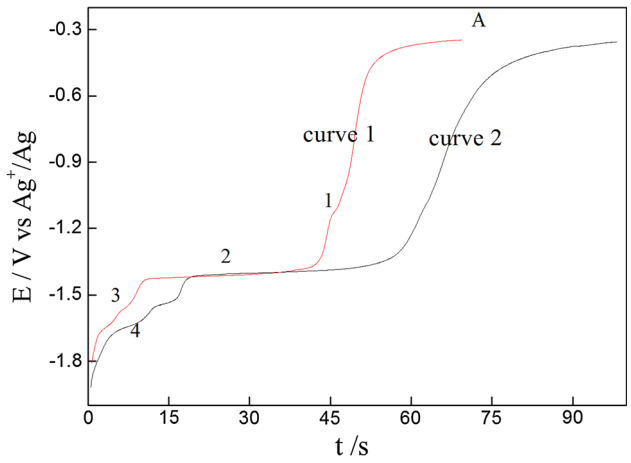

Fig. 6—Open circuit chronopotentiometry curves obtained in NaCl-KCl-$NdCl_3$ (4 wt pct) melt at 988 K (715 °C) on a Cu wire electrode (curve 1) (S = 0.32 cm^2) after potentiostatic electrolysis at −2.0 V for 30 s, and on a Cu plate electrode (curve 2) (S = 1.00 cm^2) after potentiostatic electrolysis at −2.0 V for 10 s, respectively.

B. *Reduction Behavior of Nd^{3+} in NaCl-KCl-$CuCl_2$ Melt on W and Cu Electrodes*

Figure 3 illustrates the cyclic voltammograms obtained at a W electrode (S = 0.32 cm^2) in NaCl-KCl-1 wt pct $CuCl_2$-2 wt pct $NdCl_3$ melt at different reversal potentials at 988 K (715 °C). Four pairs of well-defined signals A/A′, II/II′, III/III′, and IV/IV′ are detected. In the cathodic sense, the cathode current starts to increase from about −0.33 V, peaking at about −0.40 V (signal A), which is caused by the reduction of Cu^{2+} to Cu. The corresponding anodic signal A′ is related to the dissolution of Cu. From Figure 1, the oxidation of Nd is at about −1.82 V; therefore, the signals II′, III′, and IV′ at about −1.41, −1.54, and −1.62 V between the oxidation potential of Cu and Nd are ascribed to the dissolution of Cu-Nd intermetallic compounds in the melt.[21] The corresponding cathodic signals II, III, and IV correspond to the formation of Cu-Nd intermetallic compounds, which are formed by the underpotential deposition of Nd^{3+} on the Cu-coated W electrode, respectively. Moreover, after the signal II′, a weak signal I′ is observed corresponding to the dissolution of a Cu-Nd intermetallic compound. In NaCl-KCl-$CuCl_2$-$NdCl_3$ melts, the formation mechanism of Nd-Cu alloys obtained on the W electrode involves the steps described as follows:

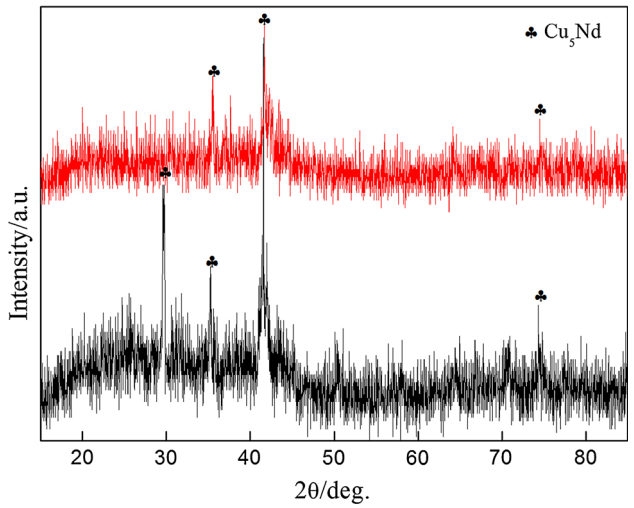

Fig. 7—XRD patterns of deposits obtained on Cu electrodes at 988 K (715 °C) under galvanostatic electrolysis at −0.5 A cm^{-2} for 2 h in NaCl-KCl melt containing $NdCl_3$ 2 wt pct (A) and 4 wt pct (B), respectively.

$$y\mathrm{Cu(II)} + 2y\mathrm{e}^- = y\mathrm{Cu(0)}; \quad [1]$$

$$x\mathrm{Nd(III)} + y\mathrm{Cu(0)} + 3x\mathrm{e}^- = \mathrm{Nd}_x\mathrm{Cu}_y. \quad [2]$$

When Cu is used as a working electrode, in NaCl-KCl-1 wt pct $CuCl_2$-2 wt pct $NdCl_3$ melt (Figure 4), in the electrochemical window, apart from the signals A/A′ relating to the formation/dissolution of metal Cu in the melt, only two pairs of well-defined signals II/II′ and III/III′ ascribed to the formation/dissolution of Cu-Nd intermetallic compounds are observed at 988 K (715 °C). The signals corresponding to the formation/dissolution of Nd are not detected, because in the cathodic process the concentration of Nd^{3+} ions on the surface Cu electrode is close to zero because of the formation of Cu-Nd alloy, and as a result, no free Nd^{3+} ions exist.

C. *Reduction Behavior of Nd^{3+} in NaCl-KCl Melt on Cu Electrodes*

To further study the Cu-Nd intermetallic compound formation, we investigated the cyclic voltammograms obtained at 988 K (715 °C) in NaCl-KCl-4 wt pct $NdCl_3$ on a Cu wire (dotted line) and plate (solid line) electrodes, respectively (see Figure 5). In the solid line, four pairs of signals I/I′, II/II′, III/III′, and IV/IV′ are detected. They correspond to the formation/dissolution of four different Cu-Nd intermetallic compounds. In the dotted line, for

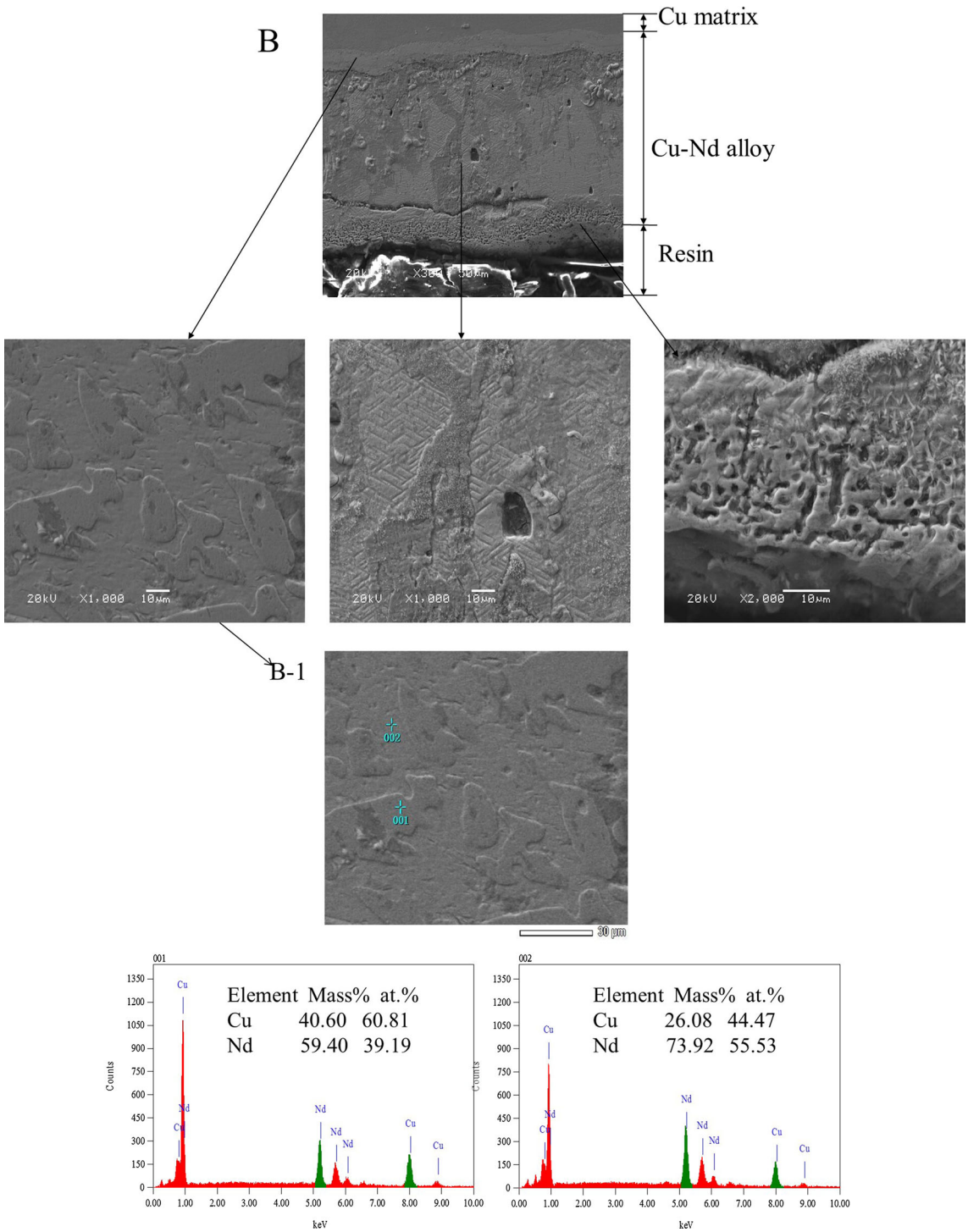

Fig. 8—SEM micrograph of a cross section of a Cu electrode at 988 K (715 °C) after galvanostatic electrolysis at −0.5 A cm^{-2} for 2 h in NaCl-KCl melt containing $NdCl_3$ 4 wt pct (B); EDS analysis of the innermost alloy layer (B-1).

the Cu wire electrode, the intensity of signal I′ become much weaker, because the formation rate of the Cu-Nd intermetallic compound (signal I) is slow in NaCl-KCl-$NdCl_3$ melt system. In NaCl-KCl-$NdCl_3$ melts, the formation mechanism corresponding to the formation of Nd-Cu alloys obtained on Cu electrode involves one step described as follows:

$$x\mathrm{Nd(III)} + y\mathrm{Cu}(0) + 3x\mathrm{e}^{-} = \mathrm{Nd}_x\mathrm{Cu}_y.$$

Figure 6 elucidates open circuit chronopotentiometry curves of NaCl-KCl-$NdCl_3$ (4 wt pct) melt obtained on Cu wire (curve 1) and plate (curve 2) electrodes at 988 K (715 °C). In this method, potentiostatic electrolysis was

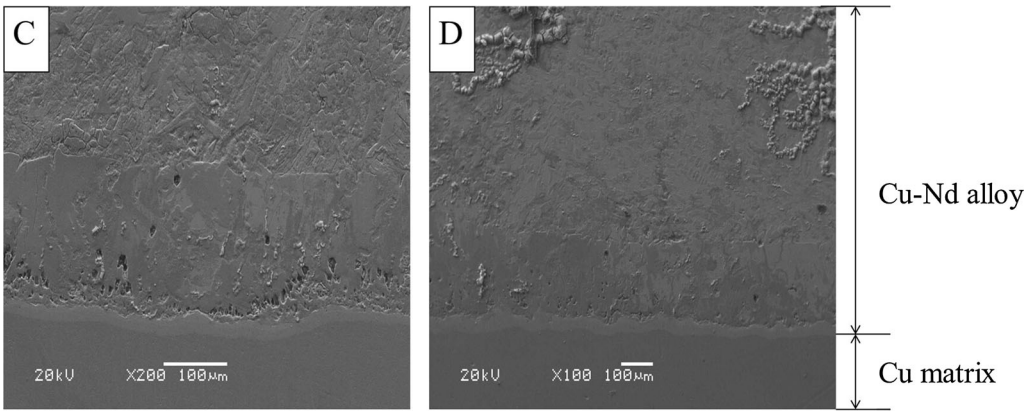

Fig. 9—SEM micrograph of a cross section of Cu electrodes at 1143 K (870 °C) after galvanostatic electrolysis in NaCl-KCl-$NdCl_3$ 4 wt pct melt at -0.5 A cm^{-2} for 4 h (sample C) and 6 h (sample D), respectively.

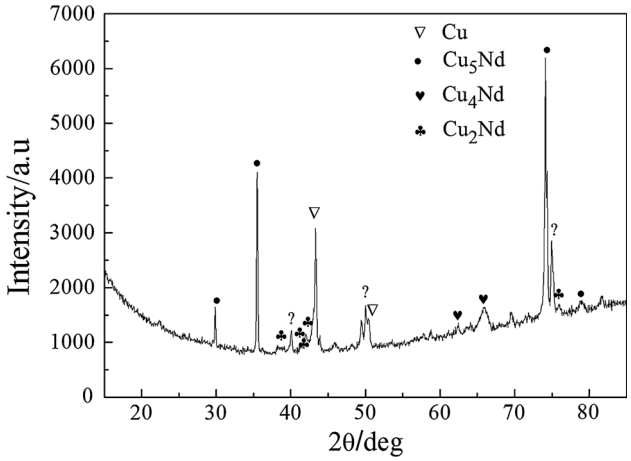

Fig. 10—XRD pattern of alloy obtained at the bottom of the crucible after galvanostatic electrolysis at -0.5 A cm^{-2} for 6 h at 1143 K (870 °C) in NaCl-KCl-$NdCl_3$ 4 wt pct melt (sample E).

employed to deposit Nd on a Cu electrode. The deposited Nd diffuses into the Cu electrode and the electrode potential gradually shifted to more positive values. During this process, a potential plateau is observed when the composition of the electrode surface is within the range of a two-phase coexisting state. In curve 1, apart from potential plateau A, corresponding to abandon the potential of Cu wire, three plateaus (plateaus 2 to 4) are observed. In curve 2, apart from plateaus A, 2 to 4, a new plateau (plateau 1) is detected. The results are in good agreement with those obtained in the anodic direction of cyclic voltammograms in Figure 5. Plateaus 1, 2, 3, and 4 are related to the two-phase coexisting states of: (1) intermetallic compound I and Cu; (2) intermetallic compounds II and I; (3) intermetallic compounds III and II; (4) intermetallic compounds IV and III, respectively. According to the subsequent XRD patterns of Nd-Cu alloys, the two-phase coexisting states of plateaus 1 to 4 can be identified as:

$$\text{Plateaus 1}: \ Cu_5Nd \ \rightarrow \ 5Cu + Nd^{3+};$$

$$\text{Plateaus 2}: \ 5Cu_4Nd \ \rightarrow \ 4Cu_5Nd + Nd^{3+};$$

$$\text{Plateaus 3}: \ 2Cu_2Nd \ \rightarrow \ Cu_4Nd + Nd^{3+};$$

$$\text{Plateaus 4}: \ 2CuNd \ \rightarrow \ Cu_2Nd + Nd^{3+}.$$

D. *Preparation of Cu-Nd Alloys on Cu Electrode*

Cu-Nd alloys were prepared *via* galvanostatic electrolysis on a Cu electrode in NaCl-KCl-$NdCl_3$ melt at 988 K (715 °C). Figure 7 displays XRD pattern of the surface of deposits obtained on Cu electrodes at 988 K (715 °C) under galvanostatic electrolysis at -0.5 A cm^{-2} for 2 hours in NaCl-KCl melt containing $NdCl_3$ 2 wt pct (A) and 4 wt pct (B), respectively. The observed diffraction peaks were identified as Cu_5Nd phase. The diffraction peaks of Cu matrix were not detected. It indicates that the whole surface of working electrode is coated with Cu_5Nd alloy film, and the X-ray does not reach the Cu substrate.[22] The intensity of those Cu_5Nd diffraction peaks is rather weak, which is due to: (i) the existence of crystal defects in Cu_5Nd alloy during formation; (ii) the attached Cu_5Nd alloy film being very thin on the Cu electrode.

Figure 8 shows SEM micrograph of a cross section of a Cu electrode at 988 K (715 °C) after galvanostatic electrolysis at -0.5 A cm^{-2} for 2 hours in NaCl-KCl melt containing $NdCl_3$ 4 wt pct. Alloy films are observed, which are divided into three obvious layers. The innermost alloy layer is rather compact with a smooth surface. To examine the distribution of the copper and neodymium elements, the EDS quantitative analysis was employed. The EDS results of the points labeled 001 and 002 taken from the innermost alloy layer (see Figure 8, B-1) indicate that the layer is composed of Cu and Nd.

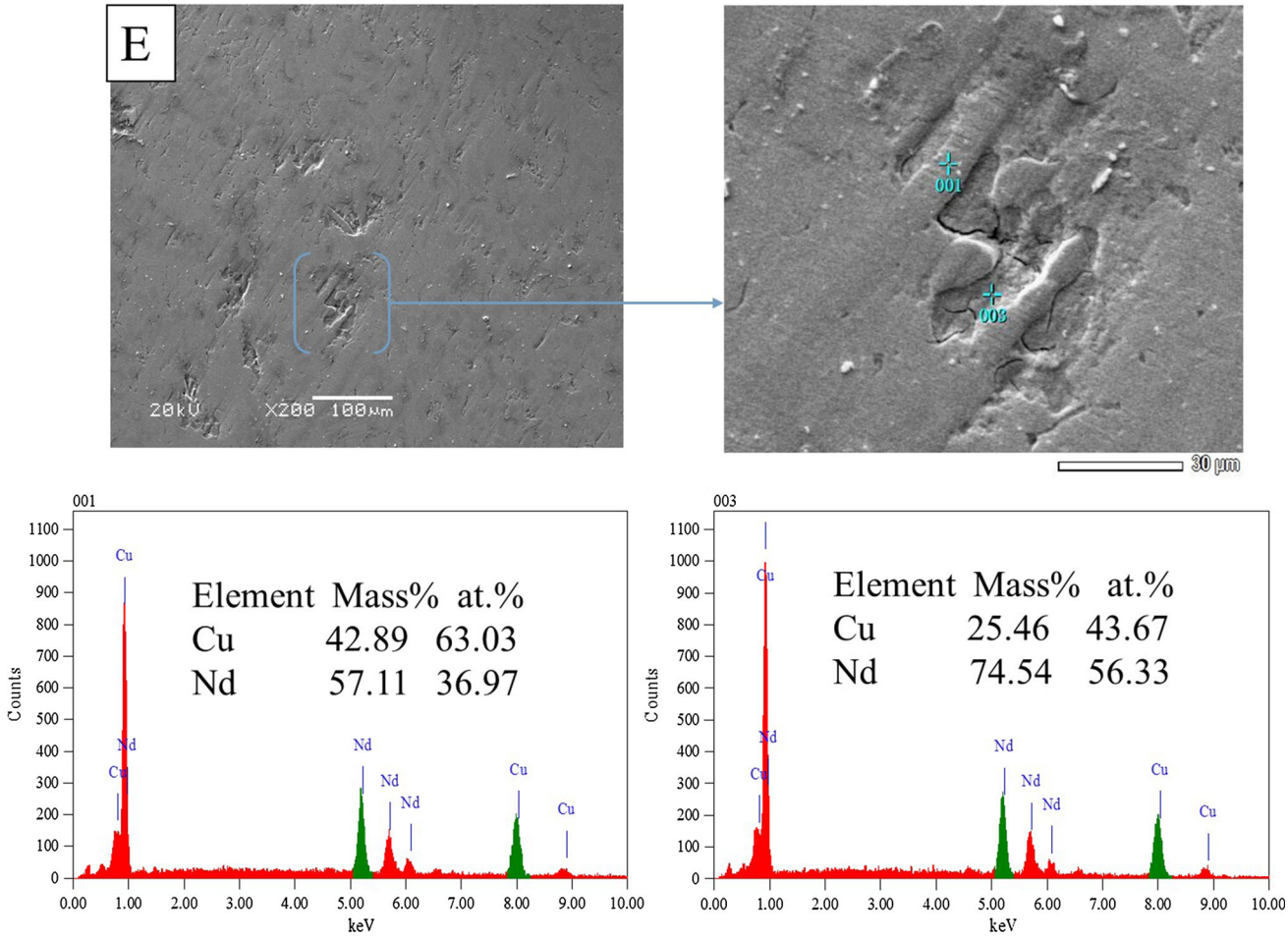

Fig. 11—SEM micrograph and EDS analysis of alloy obtained at the bottom of the crucible after galvanostatic electrolysis at 1143 K (870 °C) in NaCl-KCl-$NdCl_3$ 4 wt pct melt at −0.5 A cm^{-2} for 6 h (sample E).

To further study the Cu-Nd alloy formation, we performed a series of electrolysis at 1143 K (870 °C). Figure 9 illustrates SEM micrograph of a cross section of Cu electrodes after galvanostatic electrolysis in NaCl-KCl-$NdCl_3$ 4 wt pct melt at −0.5 A cm^{-2} for 4 hours (sample C) and 6 hours (sample D), respectively. The alloy film in sample C is divided into three obvious alloy layers, while in sample D, only two obvious alloy layers are present. After galvanostatic electrolysis at −0.5 A cm^{-2} for 6 hours in NaCl-KCl-$NdCl_3$ 4 wt pct melt, an interesting phenomenon occurs. At the bottom of the crucible, a spherical alloy (sample E) was obtained. Figure 10 shows the XRD pattern of alloy obtained at the bottom of the crucible. The Cu, Cu_5Nd, Cu_4Nd, and Cu_2Nd phases are identified. Moreover, there are some unknown diffraction peaks that could not be identified by current XRD database, which are thought to be related to other Cu-Nd intermetallic compounds. Therefore, the SEM with EDS quantitative analysis was adopted to analyze the phase constitution of alloy. Figure 11 displays the SEM images and EDS quantitative analysis data of sample E obtained at the bottom of the crucible. The surface of the alloy is rough (see SEM images). And some ribbon-like precipitates are observed. The EDS results of the points labeled 001 and 003 taken from sample E indicate that the layer is composed of Cu and Nd, with the atom percentage ratios Cu/Nd at about 1.7 and 0.78, respectively. Therefore, the precipitated Cu-Nd intermetallic compound is thought to be Cu_2Nd and CuNd phases, when the measurement error is taken into account. Since the current XRD database lacks the JCPDS of CuNd phase, therefore, the unknown diffraction peaks in XRD patterns (in Figure 10) might be related to the CuNd phase. Liquid compounds easily sink to the bottom of the crucible and keep the surface of the cathode free of diffusion layer; therefore, it can enhance the extraction rate.[3,17]

IV. CONCLUSION

On a W electrode, in NaCl-KCl melt, the reduction of Nd^{3+} ions is *via* a one-step process: $Nd^{3+} + 3e^- \rightarrow Nd$; with the assistance of $CuCl_2$, Nd^{3+} ions were reduced at more positive potentials. On a Cu electrode, four Cu-Nd intermetallic compounds were detected. Cu-Nd alloys were prepared on Cu electrode at 988 K (715 °C). Only Cu_5Nd phase was identified by XRD. SEM with EDS results suggest that the alloy film is divided into three

obvious layers. At 1143 K (870 °C), the obtained alloy film was much thicker. With the increase of electrolysis time, a globate Cu-Nd alloy was obtained at the bottom of the crucible. Cu, Cu_5Nd, Cu_4Nd, Cu_2Nd, and CuNd phases are identified by XRD and EDS quantitative analysis. The liquid alloy formation keeps the surface of the cathode free of diffusion layer, which facilitates the extraction of Nd from the melt.

ACKNOWLEDGMENTS

The work was financially supported by the Key Laboratory of Superlight Materials and Surface Technology (Harbin Engineering University), Ministry of Education, the National Natural Science Foundation of China (91326113, 91226201, and 51574097), the Science Foundation of Heilongjiang Province (LC20160 18), the Fundamental Research Funds for the Central Universities (HEUCF2016012), the Foundation for University Key Teacher of Heilongjiang Province of China and Harbin Engineering University (1253G016 and HEUCFQ1415), and the Scientific Research and Special Foundation Heilongjiang Postdoctoral Science Foundation (LBH-Q15019, LBH-Q15020, and LBH-TZ0411).

REFERENCES

1. M. Salvatores: *Nucl. Eng. Des.*, 2005, vol. 235, pp. 805–16.
2. M. Salvatores and G. Palmiotti: *Prog. Part. Nucl. Phys.*, 2011, vol. 66, pp. 144–66.
3. P. Taxil, L. Massot, C. Nourry, M. Gibilaro, P. Chamelot, and L. Cassayre: *J. Fluor. Chem.*, 2009, vol. 130, pp. 94–101.
4. D. Hudry, I. Bardez, A. Rakhmatullin, C. Bessada, F. Bart, S. Jobic, and P. Deniard: *J. Nucl. Mater.*, 2008, vol. 381, pp. 284–89.
5. T.R. Griffiths, V.A. Volkovich, S.M. Yakimov, I. May, C.A. Sharrad, and J.M. Charnock: *J. Alloy. Compd.*, 2006, vol. 418, pp. 116–21.
6. K. Fukasawa, A. Uehara, T. Nagai, T. Fujii, and H. Yamana: *J. Nucl. Mater.*, 2011, vol. 414, pp. 265–69.
7. J. Serp, P. Chamelot, S. Fourcaudot, R.J.M. Konings, R. Malmbeck, C. Pernel, J.C. Poignet, J. Rebizant, and J.P. Glatz: *Electrochim. Acta*, 2006, vol. 51, pp. 4024–32.
8. A. Novoselova and V. Smolenski: *Russ. J. Electrochem.*, 2013, vol. 49, pp. 931–37.
9. G. DeCórdoba, A. Laplace, O. Conocar, J. Lacquement, and C. Caravaca: *Electrochim. Acta*, 2008, vol. 54, pp. 280–88.
10. K. Fukasawa, A. Uehara, T. Nagai, T. Fujii, and H. Yamana: *J. Alloy. Compd.*, 2011, vol. 509, pp. 5112–18.
11. P. Masset, R.J.M. Konings, R. Malmbeck, J. Serp, and J.P. Glatz: *J. Nucl. Mater.*, 2005, vol. 344, pp. 173–79.
12. Y.D. Yan, Y.L. Xu, M.L. Zhang, Y. Xue, W. Han, Y. Huang, Q. Chen, and Z.J. Zhang: *J. Nucl. Mater.*, 2013, vol. 433, pp. 152–59.
13. A. Novoselova and V. Smolenski: *Electrochim. Acta*, 2013, vol. 87, pp. 657–62.
14. K. Yasuda, S. Kobayashi, T. Nohira, and R. Hagiwara: *Electrochim. Acta*, 2013, vol. 92, pp. 349–55.
15. C. Hamel, P. Chamelot, and P. Taxil: *Electrochim. Acta*, 2004, vol. 49, pp. 4467–76.
16. E. Stefanidaki, C. Hasiotis, and C. Kontoyannis: *Electrochim. Acta*, 2001, vol. 46, pp. 2665–70.
17. C. Nourry, L. Massot, P. Chamelot, and P. Taxil: *J. Appl. Electrochem.*, 2009, vol. 39, pp. 927–33.
18. M. Gibilaro, L. Massot, P. Chamelot, and P. Taxil: *J. Nucl. Mater.*, 2008, vol. 382, pp. 39–45.
19. P. Chamelot, L. Massot, C. Hamel, C. Nourry, and P. Taxil: *J. Nucl. Mater.*, 2007, vol. 360, pp. 64–74.
20. Y. Castrillejo, M.R. Bermejo, E. Barrado, A.M. Martínez, and P. Díaz Arocas: *J. Electroanal. Chem.*, 2003, vol. 545, pp. 141–57.
21. M. Gibilaro, L. Massot, P. Chamelot, and P. Taxil: *Electrochim. Acta*, 2009, vol. 54, pp. 5300–06.
22. H. Konishi, T. Nohira, and Y. Ito: *Electrochim. Acta*, 2002, vol. 47, pp. 3533–39.